10 Mar 1998, 2:30 pm - 5:30 pm

Effect of Smear Due to Vertical Drains on the Behaviour of Two Embankments Constructed on Soft Clays

B. Indraratna
University of Wollongong, NSW, Australia

I. W. Redana
University of Wollongong, NSW, Australia

Proceedings: Fourth International Conference on Case Histories in Geotechnical Engineering, St. Louis, Missouri, March 9–12, 1998.

EFFECT OF SMEAR DUE TO VERTICAL DRAINS ON THE BEHAVIOUR OF TWO EMBANKMENTS CONSTRUCTED ON SOFT CLAY

B. Indraratna
University of Wollongong
NSW, Australia 2522

I W. Redana
University of Wollongong
NSW, Australia 2552

ABSTRACT

2.04

This paper describes the methodology to include the effect of smear in the prediction of settlements beneath two embankments stabilized with vertical drains. The extent of smearing around the drains was studied using a detailed analytical formulation developed by the authors and used in conjunction with the finite element code, CRISP. The smear zone propagation around vertical drains was studied in the laboratory using a large radial drainage consolidometer. The case histories selected in this study include (a) embankment stabilized with vertical sand drains at a Naval Dockyard, Thailand, and (b) embankment stabilized with vertical band drains in soft Muar clay, Malaysia. It may be concluded from this study that the inclusion of smearing improves the settlement predictions significantly. The numerical results indicate that the extent of smearing is mainly dependent upon the magnitude of horizontal permeability and the drain geometry.

KEYWORDS

clays, finite element method, settlement, smear effect, smear zone, vertical drains

INTRODUCTION

This paper describes the effect of smearing due to vertical drains installed beneath embankments constructed on soft clay. The first embankment described in this study was constructed in soft Bangkok clay, Thailand. The trial embankment was stabilized under three different ground improvement schemes. Two sections of the embankment were stabilized with vertical sand drains with a drain spacing of 1.5 and 2.5 m to a depth of 17 m. The last section of the embankment (control section) was built without any foundation improvement. The second embankment was constructed on soft Muar clay, Malaysia. The soft clay foundation was stabilized with vertical band drains with drain spacing of 1.3 m to a depth of 18 m. In both case histories, the mandrel driven installation of vertical drains was responsible for smearing around the drains.

The main objective of this study was to evaluate the effect of smearing in the laboratory, and to model this effect both in the laboratory and in the field using 2-D finite element code CRISP. The sub soil is modelled according to the modified Cam-clay theory. The role of permeability on the extent of smearing was studied using an analytical formulation developed by the authors. The effect of smear was modelled by converting a single axisymmetric drain into an equivalent plane strain drain wall. The vertical drain system could be converted into equivalent parallel drain walls by adjusting the spacing of the drains and the coefficient of permeability of the soil (Indraratna and Redana,

1997). The transformed permeability coefficient was then incorporated in the finite element code, CRISP.

MODELLING OF PLANE STRAIN SOLUTION

Theory of consolidation of vertical drains under axisymmetric condition is described by Hansbo (1981). Following Hansbo's theory, Indraratna and Redana (1997) showed that if the radius of the influence zone of a single drain (R) is taken to be the same as the width (B) in plane strain (Fig. 1) then the converted plane strain ratio of the horizontal smear zone permeability, k'_{hp} to the undisturbed permeability k_{hp} is given by:

$$\frac{k'_{hp}}{k_{hp}} = \frac{\beta}{\left[\ln\left(\frac{n}{s}\right)+\left(\frac{k_h}{k'_h}\right)\ln(s)-0.75-\alpha\right]} \quad (1a)$$

where, the geometry parameters are given by:

$$\alpha = \frac{2}{3}-\frac{4b_s^3}{3B^3}+\frac{2b_s^2}{B^2}-\frac{2b_s}{B} \quad (1b)$$

$$\beta = \frac{b_s^2}{B}-\frac{b_s^3}{3B^3}-\frac{2b_w^3}{3B^3}-\frac{2b_w b_s}{B^2}+\frac{b_w^2}{B^2}+\frac{b_w^2 b_s}{B^3} \quad (1c)$$

If both smear and well resistance are ignored, then the simplified ratio of plane strain to axisymmetric horizontal permeability, k_h is represented by:

$$\frac{k_{hp}}{k_h} = \frac{0.67}{[\ln(n)-0.75]} \quad (2)$$

The converted half width of drain (b_w) and the half width of smear zone (b_s) in plane strain is given by:

$$b_w = \frac{\pi r_w^2}{2S} \text{ and } b_s = \frac{\pi r_s^2}{2S} \quad (3a)$$

for drains in a square pattern, and

$$b_w = \frac{1.143\pi r_w^2}{S} \text{ and } b_s = \frac{1.143\pi r_s^2}{S} \quad (3b)$$

for drains in a triangular pattern.

In the above, $n = R/r_w$ and $s = r_s/r_w$, r_s = radius of smear, r_w = radius of drain, S = spacing of the drains, R = radius of influence of the drain, B = width of unit cell in plane strain (B=R), k_h and k'_h = horizontal coefficient of permeability outside and inside the smeared zone, respectively. The above parameters are defined diagrammatically in Fig. 1.

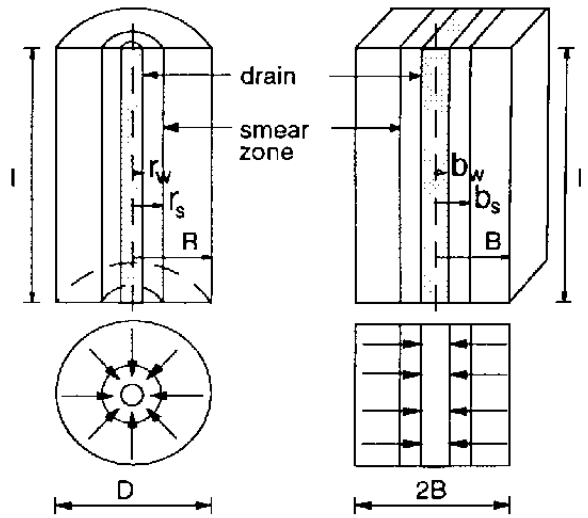

a) Axisymmetric radial flow b) Plane strain

Fig. 1 Conversion of an axisymmetric unit cell into plane strain

LABORATORY MODELLING OF SMEAR EFFECT

Laboratory testing was conducted to determine the effect of smear on the soil permeability, and to evaluate experimentally the permeability ratio k_h/k_v within and outside the smear zone. For this purpose, a large-scale consolidometer was utilized. By sampling the soil around the vertical drain, the smear zone could be quantified by the measured change in permeability. The large-scale radial drainage consolidometer consists of two half sections made of stainless steel (450 mm internal diameter), and a schematic illustration is given in Fig. 2. The cell is also equipped with a specially designed steel hoist from which a synthetic vertical drain can be inserted along the central axis of the cell. Detailed description of this consolidometer is given by Indraratna and Redana (1995).

Test Procedure

As it was not feasible to obtain one undisturbed sample for the large consolidometer apparatus, reconstituted alluvial clay from Sydney was used to make large samples. The clay size particles (<2 μm) accounted for about 40%-50% of the specimen, and particles smaller than silt size (<6 μm) constituted about 90% of the specimen. Selected geotechnical properties of the soil are: water content = 40%, Liquid Limit = 70%, Plastic Limit = 30%, unit weight = 17 kN/m^3, and specific gravity = 2.6. On the basis of the Casagrande Plasticity chart, the reconstituted clay could be categorized as CH (high plasticity clay).

Clay was thoroughly mixed with water, before placing it inside the large cylinder. Subsequently, the soil was compacted in layers, and an initial preconsolidation pressure of 20 kPa was applied prior to the installation of the central drain. The vertical sand drain was installed in the center of specimen using a specially designed pipe mandrel (50 mm diameter and 2 mm thickness) and hoist representative of a typical prototype field system. The sand poured into the pipe was lightly compacted while withdrawing the mandrel. Separate samples were prepared in the large-scale consolidometer with the central drain, and were loaded axially in increments of 50, 100, and 200 kPa to promote radial consolidation. After installing the vertical drain and subsequent loading, small specimens (50 mm in diameter) were recovered from different locations within the cell at known radii using a tube sampler (Fig. 2). The specimens were subjected to one-dimensional consolidation using standard oedometers. The measured compressibility and permeability characteristics of the smear zone around the drain were different from the rest of the clay which was unaffected by the drain installation (Fig. 2b).

Variation of Permeability Ratio, k_h/k_v

The magnitudes of the coefficients of permeability k_v and k_h were calculated by Terzaghi 1D consolidation theory, where the coefficients of consolidation (c_v and c_h) were determined on the basis of the Casagrande 'log time' method. The change in k_h/k_v ratio along the radial distance from the central drain is plotted in Fig. 3. The value of k_h' / k_v' in the smear zone varies between 0.9 and 1.3 with an average of 1.15. Hansbo (1987) argued that for extensive smearing, the ratio k_h' / k_v' could approach 1. The current experimental results certainly seem to be in agreement. For the applied range of consolidation pressures, the ratios of k_h/k_v were observed to vary between 1.4 and 1.9 (average of 1.63) in the undisturbed zone. As shown in Fig. 3, the extent of smeared zone can be estimated to be around 100 mm from the central drain.

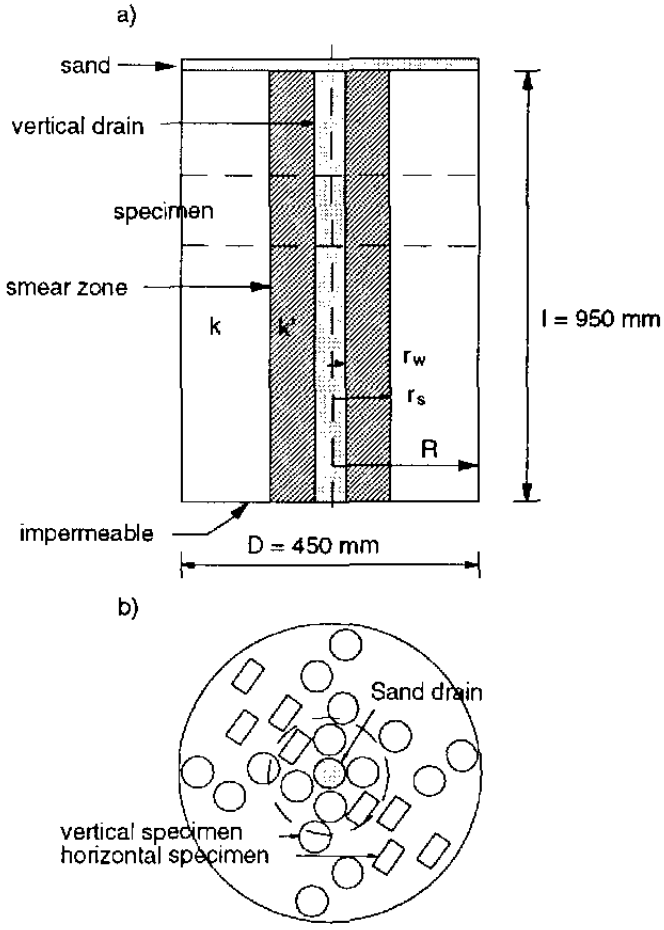

Fig. 2 a) Schematic section of the test equipment showing the central drain and associated smear and b) locations of small specimens obtained to determine the consolidation and permeability characteristics

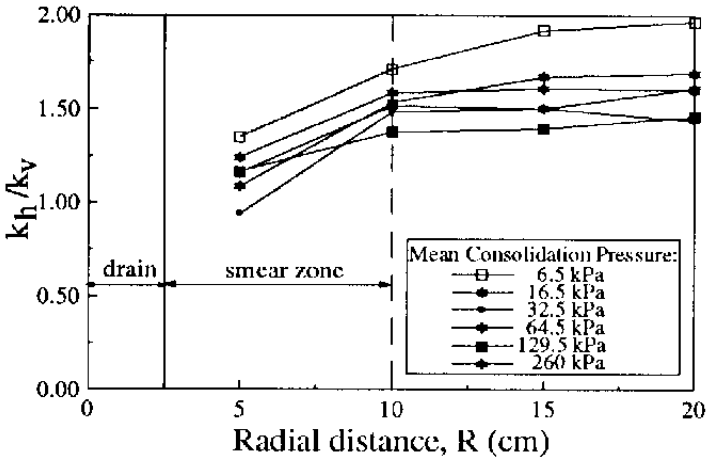

Fig. 3 Ratio of k_h/k_v along the radial distance from the central drain.

Numerical Modelling of Settlements

The settlement behaviour of clay under loading was predicted using the analytical approach proposed by Hansbo (1981), and by the plane strain finite element technique. The discretised finite element mesh for the soil cell (Fig. 4) is composed of 6-node linear strain triangular (LST) elements with three pore pressure nodes. The settlements were calculated on the basis of the modified Cam-clay theory (Roscoe and Burland, 1969) and coupled Biot-consolidation model incorporated in CRISP92 software. The clay layer is characterized by drained conditions at the upper boundary only. The excess pore water pressures were set to zero along the drain boundaries to simulate complete dissipation, and also, the effect of well resistance was neglected. Tables 1 and 2 summarize the soil properties of the clay tested in the large-scale consolidometer, and the stress levels varying with depth within the apparatus, respectively. The definitions of all parameters are listed in the Notation at the end of the paper.

The finite element predictions, Hansbo (1981) theory and the laboratory results are compared in Fig. 5. Hansbo (1981) theory underestimates settlements particularly during the final loading stage, mainly because of the assumption of the ratio of vertical to horizontal permeability being unity throughout the smear zone. The finite element analysis incorporating the laboratory based permeability ratios provides a good agreement with the measured settlements. If the effect of smear is not included in the predictions, the conventional time-settlement curve overestimates the settlements substantially (Fig. 5).

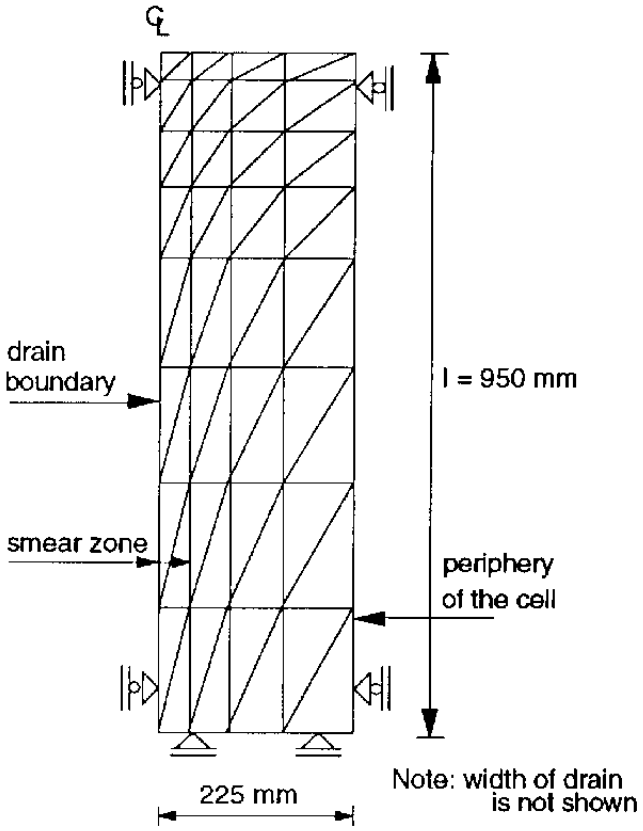

Fig. 4 Finite element discretization for plane strain analysis of the soil in large-scale consolidometer

TABLE 1. Soil properties tested in the large-scale consolidometer

Soil properties	value	units
κ	0.05	-
λ	0.15	-
e_{cs}	1.55	-
M	1.1	-
ν	0.25	-
γ_s	17	kN/m^3
k_h	$3.67x^{-10}$	m/s
k_v	$2.25x10^{-10}$	m/s
k_{hp}	$1.66x10^{-10}$	m/s
k'_{hp}	$1.12x10^{-13}$	m/s
C_c	0.34	-
C_r	0.14	-
σ'_p	20	kPa

TABLE 2. Stress state within the large-scale consolidometer

Depth (m)	σ'_h (kPa)	σ'_v (kPa)	u (kPa)	p'_c(kPa)
0	0	0	0	30
0.15	12	21	1.5	20
0.45	14	23	4.5	23
0.95	16	28	9.5	27

Note:
σ'_v, σ'_h = vertical and horizontal effective pressures
u = pore water pressure
p'_c = isotropic pre-consolidation pressure

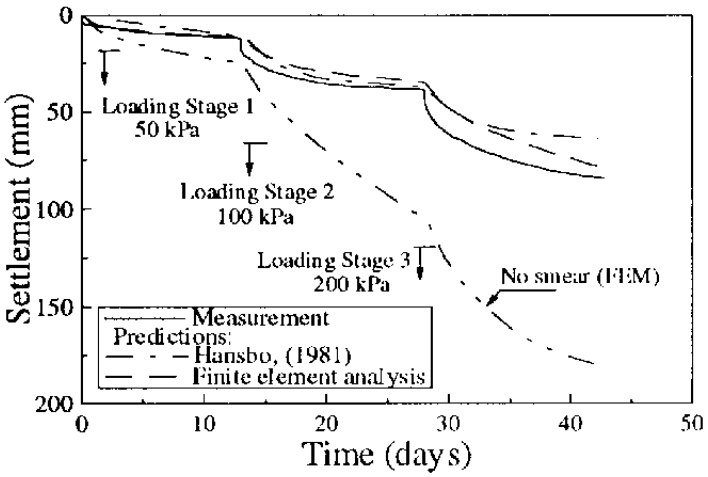

Fig. 5. Consolidation settlement of the soil stabilized with sand drain as measured in the large-scale consolidometer incorporating smear effect.

CASE HISTORY ANALYSIS 1: NAVAL DOCKYARD, BANGKOK, THAILAND.

Sub-soil Conditions

The selected case history contains the performance of sandwick drains at a Naval Dockyard test embankment in Thailand (AIT, 1977), which was located approximately 20 km south of Bangkok city, along the Chao Phraya river. The vertical drain pattern and the typical geotechnical properties of the soil layers at this location are shown in Fig. 6, where the soil layer consists of an upper layer of weathered clay to a depth of 3 m. This surface layer is underlain by soft clay, silts and sandy silt to a depth of 17.2 m, followed by a stiff clay to a depth of 25 m below the ground level. The sandwick drains consist of a hose made of a fibrous material of fair strength and of high permeability, and filled with a dry sand. The diameter of the drains was 5 cm and the drains were installed to a depth of 17 m to reach the stiff clay layer. In order to install the wicks, a casing of 7.5 diameter with a wooden plug at its lower end was pushed into the soft ground using a 2 tonne hammer. The drains were installed in a square grid with a regular spacing of 1.5 m and 2.5 m at different sections of the embankment, T1 and T2, respectively. The instrumentation scheme for monitoring settlements of the embankments was of two types, namely, the surface settlement points and subsurface settlement points. In order to monitor the porewater pressures, piezometers were installed below the test fill area and outside the fill area. The embankment loading was applied in three stages: firstly, the placing of a sand blanket of thickness 0.35 m, followed by an initial layer of fill of 1.10 m, which was then continued until a total fill height of 2.35 m was attained (Fig.6). The loading scheme of the unstabilized section (T3) of the embankment (without drains) was the same, therefore, the performance of the embankment with and without drains could be compared.

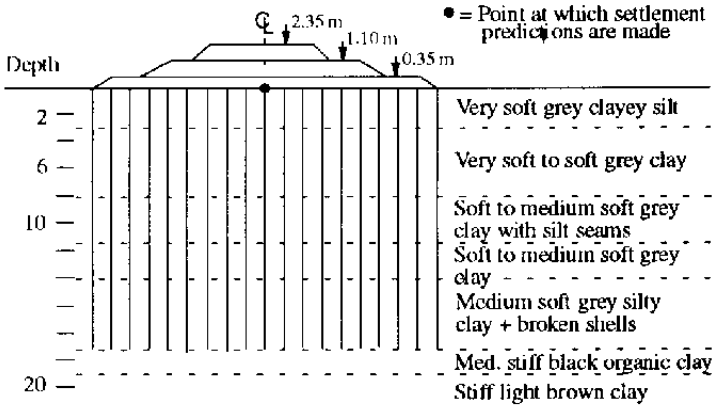

Fig. 6 Cross section through centerline of embankment with sub-soil profile at Naval Dockyard.

Numerical Analysis

The Cam-clay parameters for each soil layer and the in-situ stress levels are given in Table 3 and 4,

respectively. In order to estimate the undisturbed soil permeability, laboratory consolidation tests have been conducted on both vertically and horizontally oriented specimens (AIT, 1977). For the smear zone surrounding the drain, the horizontal permeability was assumed to be equal to 1.15 times the vertical permeability, based on the current laboratory tests conducted by the authors. The measured horizontal and vertical permeability coefficients of the undisturbed soil (k_h and k_v) and the equivalent plane strain values based on Eqs. (1) and (2) are given in Table 5.

The discretised finite element mesh near the drain boundary is shown in Fig. 7, which contains 6-node linear strain triangular (LST) elements with three pore pressure nodes. In the axisymmetric condition, the equivalent radius of sandwick drains and smear zone are $r_w = 0.05$ m and $r_s = 0.375$ m, respectively. The equivalent plane strain width of the drain and of the smear zone are as follows. For embankment T1: S=1.5 m, B=0.75 m, b_w=0.003 m and b_s=0.15m; for embankment T2: S=2.5 m, B=1.25 m b_w=0.002 m and b_s=0.09 m. The above notation of parameters is in Fig. 1.

The results of the plane strain analysis together with the measured settlements for drain spacing 1.5 m and 2.5m are plotted in Figs. 8a and 8b, respectively. The analysis based on perfect drain conditions (no smear, complete pore pressure dissipation) overpredicts the measured settlement, whereas the inclusion of smear effect significantly improves the accuracy of the predictions. However, a better prediction is obtained if the permeability of the smear zone is arbitrarily increased by a factor of about 3-5 for all sub-soil layers, representing a partially smeared condition. Increased ground permeability is not surprising, because the porosity in the field can often be larger than that of small laboratory specimens due to ground anisotropy, natural fissures, etc. As shown in Fig. 8b where the drains spacing is 2.5 m, the centerline surface settlement prediction is excellent.

TABLE 3. Cam-clay parameters used in numerical analysis

Depth (m)	κ	λ	e_{cs}	M	ν	γ_s kN/m³
0-3	0.09	0.4	3.61	0.80	0.29	16
3-8	0.09	0.87	5.06	1.10	0.31	16
8-11.5	0.09	0.48	3.35	0.90	0.29	15
11.5-14	0.09	0.30	2.79	0.88	0.26	16
14-17	0.09	0.22	2.26	0.93	0.26	17

TABLE 4. In-situ stress condition used in numerical analysis

Depth (m)	σ_{ho} (kPa)	σ_{vo} (kPa)	u (kPa)	p_c
1	9.2	14	0	14.4
3	18.6	28.4	19.6	29
8	31.7	59.3	68.7	56.2
11.5	47.8	77.5	103	77.5
14	57.3	92.9	127.5	92.9
17	68.3	114.5	156.9	113

TABLE 5. Coefficients of permeability used in numerical analysis

Depth (m)	k_h (m/s) x 10^{-10}	k_v (m/s) x 10^{-10}	Drains Spacing 1.5 m		Drains Spacing 2.5 m	
			k_{hp} (m/s) (no smear) x10^{-10}	k'_{hp} (m/s) (with smear) x10^{-12}	k_{hp} (m/s) (no smear) x10^{-10}	k'_{hp} (m/s) (with smear) x10^{-13}
0-3	457	261	156	124	123	213
3-8	20.8	11.9	7.09	5.67	5.62	9.71
8-11.5	6.46	3.69	2.20	1.76	1.74	3.01
11.5-14	4.78	2.73	1.63	1.30	1.29	2.23
14-17	2.64	1.51	0.9	0.72	0.714	1.23

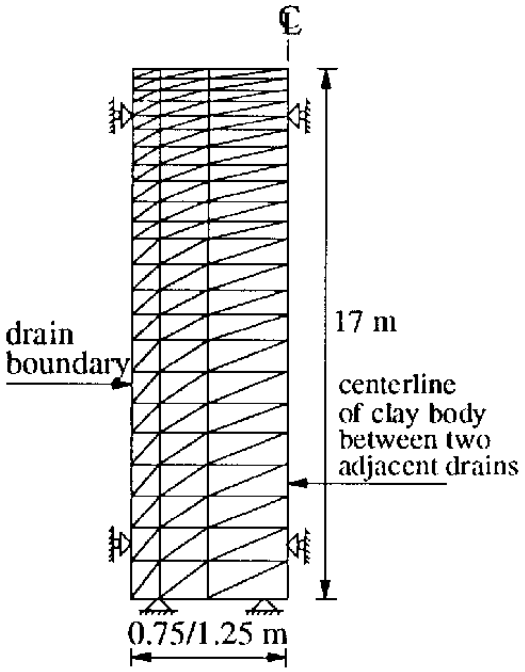

Fig. 7 Finite element mesh in the vicinity of drain at a Naval Dockyard, Thailand

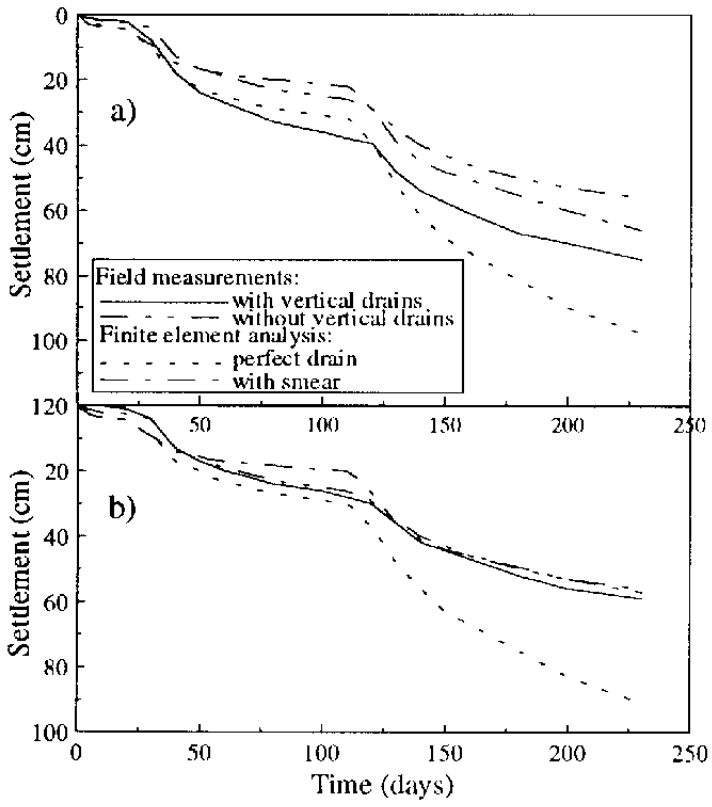

Fig. 8. Consolidation settlement at ground surface at embankment centerline at a Naval Dockyard Thailand (a) embankment T1 with drain spacing 1.5 m and (b) embankment T2 with drains spacing 2.5 m.

The predicted and measured excess pore water pressures under the centerline of the embankment at depths of 7 m below the ground surface are compared in Fig. 9. It is observed that the field measurements are in excess of the numerical predictions during Stage 1 and Stage 2 of loading, whereas the pore pressures at Stage 3 loading are generally well predicted. It is anticipated that partial clogging of some of the drains near the piezometer location (hence, retarded pore pressure dissipation) can probably be the cause of this (Indraratna et al., 1994). Another cause of error can be attributed to the fact that the nodal pore pressure points at the 7 m depth on the finite element mesh did not necessarily coincide exactly with the piezometer tips.

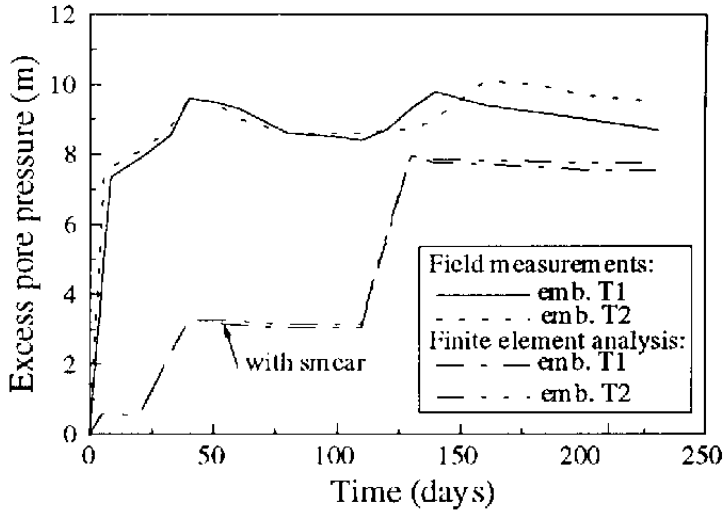

Fig. 9 Variation of excess pore water pressures at embankment centerline for piezometer at 7 m below ground level

CASE HISTORY ANALYSIS 2: MUAR CLAY, MALAYSIA

Sub-soil Conditions

This embankment was built on soft Muar clay in Malaysia. Fig. 10 shows the cross section of the embankment and the sub-soil profile beneath the embankment. The embankment was composed of compacted sandy clay having a unit weight of 20.5 kN/m^3. During Stage 1 of construction, the embankment was raised to a height of 2.57 m in 14

days. Following a rest period of 105 days, additional fill was placed (Stage 2) until the embankment reached a height of 4.74 m in 24 days. The settlements and excess pore water pressures were monitored for about 400 days (Indraratna et al., 1994).

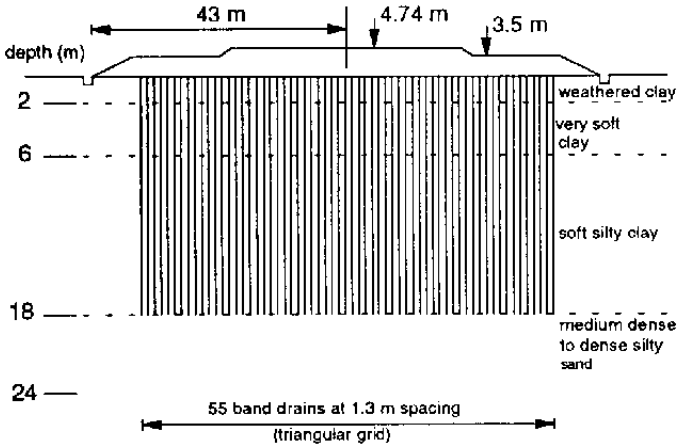

Fig. 10 Cross section through centerline of embankment with sub-soil profile

Numerical Analysis

The Cam-clay parameters for each soil layer are shown in Table 6, and the in-situ stress distribution with depth is given in Table 7. The undisturbed soil permeabilities were estimated from laboratory consolidation tests conducted on both vertically and horizontally cored specimens. In the smear zone, the horizontal permeability was assumed to be 1.15 times the vertical permeability. The measured horizontal and vertical permeability coefficients of the undisturbed soil (k_h and k_v) and the equivalent plane strain values are given in Table 8.

TABLE 6. Cam-clay parameters used in numerical analysis

Depth (m)	κ	λ	e_{cs}	M	ν	γ_s kN/m^3
0-1.8	0.06	0.16	3.10	1.19	0.29	16.5
1.8-5.5	0.06	0.16	3.10	1.19	0.31	15.0
5.5-8.	0.05	0.13	3.06	1.12	0.29	15.5
8-18	0.04	0.09	1.61	1.07	0.26	16.0

TABLE 7. In-situ stress condition used in numerical analysis

Depth (m)	σ_{ho} (kPa)	σ_{vo} (kPa)	u (kPa)	p_c
0	0	0	0	110
1.8	17.3	28.9	0	95
5.5	29.1	48.4	36.7	44
8	37.6	62.6	61.3	60
18	74.8	124.6	159.3	65

The discretized finite element mesh near the drain boundary is shown in Fig. 11, which contains 6-node linear strain triangular (LST) elements with three pore pressure nodes. The prefabricated vertical drains were installed in a triangular pattern at a spacing of 1.30 m. The equivalent drain diameter, the diameter of the axisymmetric influence zone for each drain, and the extent of the smear zone were estimated to be 70 mm, 1.365 m and 0.4 m, respectively. For the triangular pattern of vertical drains, the equivalent widths of the drain and smear zone were calculated using Eq. (3b) to give: b_w = 0.34 cm and b_s = 11 cm, respectively. Because of

TABLE 8. Coefficients of permeability used in numerical analysis

Depth (m)	k_h (m/s)	k_v (m/s)	k_{hp} (m/s) (no smear)	k'_{hp} (m/s) (with smear)
0-1.8	6.4×10^{-9}	3.0×10^{-9}	1.9×10^{-9}	7.9×10^{-12}
1.8-5.50	5.2×10^{-9}	2.7×10^{-9}	1.6×10^{-9}	7.2×10^{-12}
5.50-8.0	3.1×10^{-9}	1.4×10^{-9}	9.5×10^{-10}	3.7×10^{-12}
8.0-18.0	1.3×10^{-9}	0.6×10^{-9}	3.9×10^{-10}	1.6×10^{-12}

symmetry, it was sufficient to consider one half of the unit cell. The clay layer was characterized by drained conditions at both the upper and lower boundaries. The embankment loading was simulated by applying incremental vertical loads to the upper boundary. The excess pore water pressures were set to zero along the drain boundary to simulate complete dissipation. The effect of well resistance was neglected, and only the effect of smearing was considered using Eq. (1).

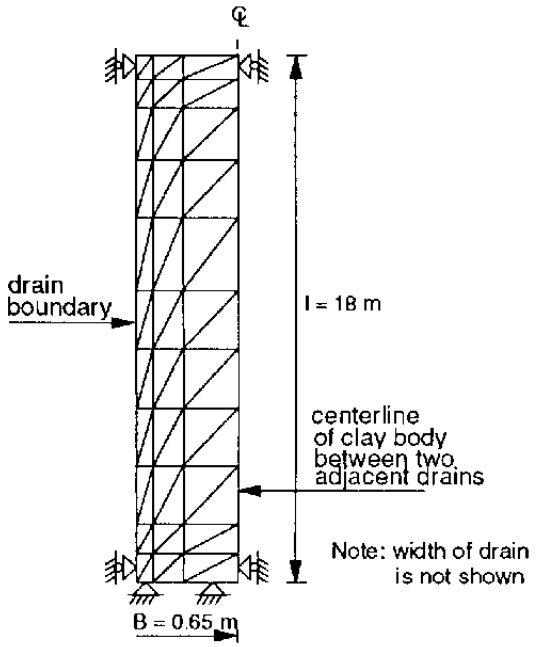

Fig. 11 Finite element mesh in the vicinity of drain

The results of the plane strain analysis together with the measured settlements are plotted in Fig. 12a. As expected, the analysis based on perfect drain conditions (no smear, complete pore pressure dissipation) overpredicts the measured settlement. The inclusion of smear effect significantly improves the accuracy of the predictions. An excellent match is again obtained if the permeability of the smear zone is arbitrarily increased by a factor of 2.5-3.0 for all sub-soil layers. As mention earlier, this is because the field permeability can often be larger than that of small laboratory specimens. The predicted and measured excess pore water pressures under the centerline of the embankment at depths of 9.1 m and 13.6 m below the ground surface are compared in Fig. 12b. The pore pressure increase during Stage 1 loading is well predicted, but the post-construction predictions (after Stage 2 loading) indicate a greater rate of pore pressure dissipation in comparison with the gradually decreasing field values.

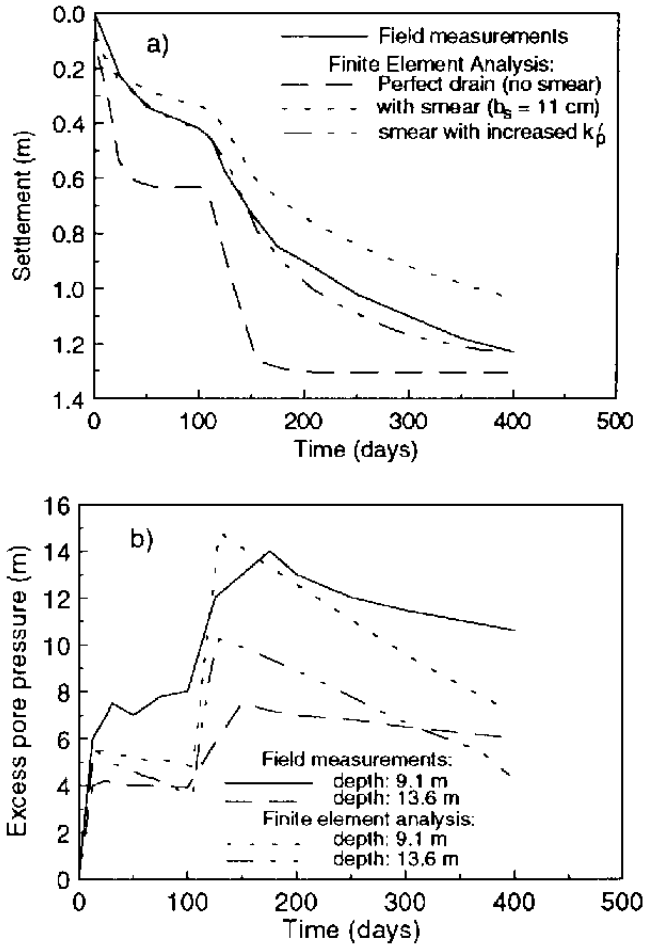

Fig 12 (a) Consolidation settlement at ground surface of embankment center; and (b) Variation of excess pore water pressures at embankment centerline for piezometer at 9.1 m and 13.6 m below ground level

CONCLUSION

This study highlighted the behaviour of soft clay foundation under embankment loading, with reference to two case histories taken from Thailand and Malaysia, respectively. The numerical analysis was extended to include the effects of smear caused by mandrel driven vertical drains. The soft clay consolidation was modelled by the modified Cam-clay theory and the coupled Biot-consolidation model.

The effect of smear was investigated in the laboratory, using a large-scale consolidometer having the facility of a central drain, promoting

radial drainage. By measuring the variation of the horizontal permeability close to and away from the centrally installed drain, the extent of the smear zone could be determined. The smear zone radius was estimated to be a factor of 4-5 times the radius of the central drain. At the drain-soil interface, the measured ratio of horizontal to vertical permeability approached unity. The inclusion of the correct variation of the permeability ratios (i.e. as a function of the radial distance from the central drain) in the finite element method is a more realistic tool for predicting settlements. The analysis of these two case histories verify that the smear effects can affect the settlements significantly. It is also pointed out that the correct prediction of excess pore pressures at the beginning of the loading stages is often difficult because of partial clogging of some drains that lead to retarded pore pressure dissipation. In contrast, the excess pore pressure and the settlements can be predicted accurately, towards the end of construction and during the post-construction period.

ACKNOWLEDGMENT

Continuing support of Prof. A. S. Balasubramaniam (AIT), in providing past field measurements is gratefully appreciated. Assistance of Dr. A. Britto (Cambridge University) on various occasions is also appreciated.

REFERENCES

Asian Institute of Technology (AIT), (1977). *Performance of sand drains in a test embankment at the Naval Dockyard site, Pom Prachul. Technical Report*, Div. of Geotechnical & Transportation Eng. AIT, Bangkok, Thailand. p. 209.

Barron, R. A. (1948). *Consolidation of fine-grained soils by drain wells*. Trans. Am. Soc. Civ. Engrs., 113, 718-742.

Britto, A.M. and Gunn, M.J. (1987). *Critical state soil mechanics via finite elements*. Chichester: Ellis Horwood, U. K, 486 p.

Hansbo, S. (1981). *Consolidation of fine-grained soils by prefabricated drains*. Proc. 10th Int. Conf. on Soil Mechanics and Foundation Engineering, Stockholm, Sweden, Publications Committee of ICSMFE (ed.), Balkema, A. A., Rotterdam, 677-682.

Indraratna, B., Balasubramaniam, A. S., and Ratnayake, P., (1994). *Performance of embankment stabilized with vertical drains on soft clay*. J. Geotech. Eng., ASCE, 120 (2), 257-273.

Indraratna, B. and Redana, I W., (1996), *Large-scale, radial drainage consolidometer with central drain facility*. Australian Geomechanics, 29, 103-105.

Indraratna, B. and Redana, I W., (1997), *Plane strain modeling of smear effects associated with vertical drains*. J. Geotech. Eng., ASCE, 123 (5), 474-478.

Roscoe, K.H., and Burland, J.B. (1968). *On the generalized stress strain behavior of wet clay*. Engineering plasticity, Cambridge Univ. Press; Cambridge, U.K., 535-609.

NOTATION

λ = the gradients of volume against log pressure relations for consolidation

κ = the gradients of volume against log pressure relations for swelling

M = slope of the critical state line based on effective stress

e_{cs} = void ratio at unit consolidation pressure

ν = Poisson's ratio

γ_s = unit weight of soil

C_c = compression index

C_r = recompression index

σ'_p = maximum past pressure